Available online at www.sciencedirect.com

ScienceDirect

Procedia Engineering 97 (2014) 871 – 880

Procedia Engineering

www.elsevier.com/locate/procedia

12th GLOBAL CONGRESS ON MANUFACTURING AND MANAGEMENT, GCMM 2014

Comparative Studies of High and Low Frequency Pulsing On the Aspect Ratio of Weld Bead in Gas Tungsten Arc Welded AISI 304L Plates

Arivarasu.M*, Devendranath Ramkumar K, Arivazhagan.N

School of Mechanical & Building Sciences, VIT University, Vellore-632014, India

Abstract

This research article presents the optimization of process parameters for pulsed current gas tungsten arc welded austenitic stainless steel AISI 304L of 4mm thickness. Investigations were carried out to study the effect of frequency with respect to penetration and bead width to penetration ratio (Aspect Ratio).Three level 4 factor Taguchi L9 orthogonal array was used to carry out the bead on plate welds. Taguchi analysis was done for main effects plot to optimize the process parameters and ANOVA was used to find the percentage contribution of each factor and their responses. The key findings of the article elucidated that full penetration with optimized aspect ratio could be achieved on employing high frequency pulsing.

Selection and peer-review under responsibility of the Organizing Committee of GCMM 2014

Keywords: Bead on weld; High Frequency Pulsing; Low Frequency pulsing; Taguchi; ANOVA

Nomenclature

I_P	-	Peak current (A)	S/N	-	Signal to noise ratio
I_B	-	Base current (A)	HI	-	Heat input in J/mm
Peak %	-	Peak current ON Percentage	P	-	Penetration
			W	-	Bead Width
frequency	-	Pulse frequency	W/P	-	Aspect ratio (AR)

* Corresponding author. Tel.: Phone: +91-9488982584; fax:+91416-2243092
E-mail address: arivarasu.m@vit.ac.in

Selection and peer-review under responsibility of the Organizing Committee of GCMM 2014
doi:10.1016/j.proeng.2014.12.362

1. Introduction

AISI 304L low carbon content austenitic stainless steel is one of the most versatile and widely used material due to its superior strength, toughness and corrosion resistance in a wide variety of applications which does not limit to aerospace, automotive, nuclear and thermal power plants, pressure vessels, petroleum refineries, cryogenic environments, pulp and paper industries, acidic medium, food processing, kitchen appliances [1-3]. Owing to the presence of low carbon content, this stainless steel is free from the chromium carbide precipitation during welding and hence sensitization effect is eliminated. It was also reported that AISI 304 L is practically immune to sigma phase formation which makes it suitable to operate even in high temperature services [3].

Majority of the fabricators prefer AISI 304L due to its excellent weldability with less metallurgical problems in the fusion welding techniques. Heat input is one of the influencing factors that affect the quality of the weldments. Many researchers addressed that the welding of AISI 304L must be carried out using an optimal heat input to avoid the deformation of the weldments and also to avoid the metallurgical effects. Giridharan et al. [4] reported that heat input has a significant impact on the bead geometry, metallurgical, mechanical and corrosion resistance properties of the welds. Similarly, Karunakaran [5] reported that the rate of heat input during welding followed by the nature of cooling has a strong influence on the grain size and phase formation. As recommended by Martin [6], the maximum heat input that can be employed for joining AISI 304L should not exceed 1.5 kJ /mm.

Yousefieh et al.[7] observed that excessive heat input during welding resulted in the formation of brittle inter metallic phases and/or the formation of coarse columnar grains which resulted in poor weld mechanical properties and adversely affected the corrosion resistance. Kou et al. [8] found that current pulsing is an effective technique to control the heat input and helps in grain refining of the weld fusion zones.

Several researchers reported the accrued benefits obtained on employing Pulsed Current Gas Tungsten Arc Welding (PCGTAW) welding that includes efficient use of arc energy, decrease in wastage of heat by conduction through base metal and thus reduced heat affected zone. Furthermore improved arc stability, lower heat input requirements, reduced residual stresses and distortion and refinement of fusion zone microstructure are the other advantages of PCGTA welding [4, 5, 9, and 10].

Further, various researchers reported the beneficial effect of current pulsing which normally result in the refined grain structure both in the weld and weld interface. This shall be attributed to the thermal cycle in which temperature goes to a peak value followed by rapid cooling in these zones [10].Hence a more controlled bead profile can be expected on employing pulsed current than the continuous current mode. It is also reported that the successful welds are usually quantified by obtaining higher penetration and lower bead width. Thus it is desirable to have lower aspect ratio (AR) in a weld, which is obtained by controlled heat input, thereby resulting in good weld properties [11]. It is also suggested that the welding conditions should be controlled to obtain slower cooling rate for adequate austenite formation and fast enough to prevent deleterious precipitation. Similarly the selection of I_P and I_B must be adequate enough to obtain desired bead contour, bead penetration and stable arc as reported by Balasubramanian et al. [12].

Babu et al. [13] pointed out the importance of using optimum pulse parameters for maximizing the beneficial effects of current pulsing. The authors employed central composite experimental design along with Hooke and Jeeve's pattern search method for optimizing PCGTAW parameters to obtain minimum fusion zone grain size and maximum tensile strength of the joint. Giridharan et al. [4] employed central composite rotatable mathematical design method for optimizing the PCGTAW parameters to achieve optimum bead geometry.

Yousefieh et al. [14] investigated the optimization of PCGTAW parameters for improving the corrosion resistance of super duplex stainless steel weld using Taguchi and ANOVA. A four parameter three level design L9 orthogonal array was chosen for the experiment. S/N ratio analysis was employed to determine the optimum parameters and ANOVA was done to identify the percentage contribution of each parameter and their response.

Giridharan et al. [4] investigated autogeneous full penetration PCGTA welding of 3 mm sheet AISI 304 L at a lower frequency of 1 Hz. In addition the authors optimized the process parameters with respect to penetration, width and aspect ratio using a quasi-Newton numerical optimization technique. Moreover, it is concluded that pulsed current is also one of the most influencing process variable in their study.

Padmanban et al. [15] reported that the pulse frequency has the greatest influence on tensile strength than other process parameters like I_P, I_B and Peak %. The frequency values employed in their study was in the range from 2 to 10 Hz. The results showed that higher tensile properties were obtained on employing 6 Hz frequency. It was deduced from the results that frequency has a vital role in obtaining high quality welds. It was emphasized to use

high frequency pulse (100 to 500 Hz) than low frequency one in order to constrict the arc cone. On deploying the arc cone, the depth of penetration could be increased and bead width would be lowered [16]. As a nutshell, high frequency current pulsing technique improves the productivity in terms of better control over the heat input and offers the possibility of higher welding speeds.

Hitherto, the investigations reported on the use of high frequency pulsing and the corresponding effects on the variables were found to be scanty. As AISI 304L has several advantages in versatile industries, this comparative study of low and high frequency current pulsing shall become inevitable. In the present research work, the effect of low and high frequency current pulsing on the depth of penetration and bead width of AISI 304 L is investigated. The process parameters were optimized using Taguchi method and determined the significance of each parameter on the responses using ANOVA.

2.1 Design of experiment using Taguchi method

In this study, a four factor three level array was used, the number of degrees of freedom (DOF) would be 8 [D.O.F = number of factors × (number of levels-1)]. If full factorial experimentation is to be employed for a 4 factor 3 level combination, then a total of 3^4=81 experiments are needed, which is tedious and time consuming. Hence Taguchi's L9 orthogonal array is used to study the main effects using 9 experiments rather than carrying out 81 experiments.

In Taguchi method, the optimum value is determined by calculating the S/N ratio of the result obtained. Signal to Noise ratio is the performance characteristic having three categories such as (i) Higher the better; (ii) lower the better; and (iii) nominal the better.

In the current study, the performance characteristics such as depth of penetration and bead width are chosen. Depth of penetration is considered to be desirable quality and bead width is identified to be the non-desirable quantity. Hence for the aspect ratio (W/P), lower the better criterion was chosen for S/N ratio analysis.

The S/N ratio equation [14] for lower the better criteria is given by

$$\frac{S}{N} = -10 \log 10 \frac{1}{n} \sum_{i=1}^{n} Yi^2 \qquad (1)$$

Where, n is the no. of repetition of an experimental combination, Yi is the performance value of i^{th} experiment.

At each level of the four factors, mean value of S/N ratio was calculated. Level with highest mean S/N value among all three levels of a factor was chosen as the optimum level of the corresponding factor.

2.2 Experimental procedure

Candidate material for this study is austenitic stainless steel AISI 304L of 4 mm thickness. Four plates of dimensions (200 mm × 100 mm × 4 mm) were cut from rolled plate. Chemical composition of the base material is represented in Table 1. Bead on welding was done on the plates by pulsed current GTAW process using Kemppi Master TIG MLS 4000. Argon gas with a flow rate of 15 lpm was used as the shielding gas. Taguchi's L9 orthogonal array was used to design the experiments in this research work. In the L9 orthogonal array, nine experiments were carried out to study the influencing weld process parameters. A total of 18 experiments were carried out to study the effect of frequency on the process variables. Out of these 18, nine experiments in each were carried out for low frequency and high frequency current pulsing. The important four parameters of PCGTAW were chosen as depicted by Yousefieh et al.[14]. The range of each process parameter levels were decided based on trial welds and the process parameters such as I_P, I_B, frequency and Peak % along with their levels used are shown in Table 2.The heat input required for

Table 1 Chemical Composition of base material

	Chemical Composition (% by Weight)								
Base Metal	C	Si	Mn	P	Ni	Nb	Mo	S	Cr
AISI 304L	0.0290	0.0300	1.37	0.0270	8.35	0.0120	0.300	0.0090	18.67

Table 2 Process parameters and their respective levels for LF- Pulsing and HF Pulsing

Factors	Peak current (I_p) A	Base current ($I_{b)}$ A	Peak %	Low Frequency (f) Hz	High Frequency (f) Hz
Level 1	240	100	40	6	150
Level 2	260	120	50	8	200
Level 3	280	140	60	10	250

each welding experiment was calculated before welding; based on the above set of process parameters to ensure that the heat input is within the permissible limit. The heat input [7] was calculated using the following equation

$$HI = \eta \times \frac{I_m \times V}{S} J/mm \quad (2)$$

In PCGTAW, mean current is considered for heat input calculation because the current is being pulsed from a higher peak value to a lower base value at a particular frequency. The mean current I_m is calculated using the equation

$$I_m = \frac{(I_P \times t_p) + (I_b \times t_b)}{t_p + t_b} \quad (3)$$

Where, I_P is the peak current, I_b is the base current, t_p is the peak current duration and t_b is the base current duration. Based on the different levels of parameters designed using L9 orthogonal array, PCGTA welding was carried out on the 304L plates at low and high frequency. The low frequency levels of 6, 8, and 10 Hz and high frequency levels of 150, 200 and 250 Hz were employed in the study. The process parameter combinations for the LF and HF are listed in Table 3 and 4. Samples of size 25 mm in length were cut using wire EDM from all the weld beads for examining the cross section and to analyze the bead profile. The samples which were cut was polished using standard metallographic procedure. The polished samples were etched using aquaregia (15 ml HCl + 5 ml HNO_3) and examined through optical macroscope for bead profile. Image tool version 3.00 software was used to measured Depth of penetration and bead width.

Table 3 Taguchi L9 Orthogonal array and Experimental results of LF-pulsing for the bead geometry their corresponding S/N values and heat inputs

Exp No.	Peak Current I_p(A)	Base Current I_b(A)	Peak %	f (Hz)	Volts (V)	P (mm)	W (mm)	Aspect Ratio (W/P)	S/N values for Aspect ratio	Heat input J/mm
1	240	100	40	6	13.5	1.96	11.00	5.61	-14.9827	505
2	240	120	50	8	16.0	3.90	13.7	3.51	-10.9131	691
3	240	140	60	10	14.0	3.00	13.03	4.34	-12.7564	672
4	260	100	50	10	15.5	3.05	12.75	4.18	-12.4242	669
5	260	120	60	6	15.0	2.54	11.93	4.69	-13.4361	734
6	260	140	40	8	15.0	1.98	10.64	5.37	-14.6055	676
7	280	100	60	8	15.4	3.52	13.73	3.90	-11.8225	768
8	280	120	40	10	15.6	3.06	12.93	4.23	-12.5175	688
9	280	140	50	6	16.0	2.83	13.87	4.90	-13.8058	806

Table 4 Taguchi L9 Orthogonal array and Experimental results of HF-pulsing for the bead geometry and corresponding S/N ratios and heat inputs

Exp No.	Peak Current I_p(A)	Base Current I_b(A)	Peak %	f (Hz)	Volts (V)	P (mm)	W (mm)	Aspect Ratio (W/P)	S/N Values for Aspect Ratio	Heat input J/mm
1	240	100	40	150	16.0	1.73	7.81	4.51	-13.0920	499
2	240	120	50	200	16.0	1.98	9.88	4.98	-13.9618	576
3	240	140	60	250	15.8	2.64	11.15	4.22	-12.5134	632
4	260	100	50	250	16.0	2.17	10.61	4.88	-13.7851	576
5	260	120	60	150	16.0	4.03	13.29	3.29	-10.3643	652
6	260	140	40	200	14.5	1.41	9.16	6.49	-16.2535	545
7	280	100	60	200	15.3	2.24	11.80	5.26	-14.4326	636
8	280	120	40	250	15.0	1.84	10.38	5.64	-15.0275	552
9	280	140	50	150	15.0	2.42	12.51	5.16	-14.2688	630

3. Experimental results

3.1 Macrostructure examination

The bead on plate welds showed the acceptable weld quality with good weld beads. The weld bead geometry obtained from low and high frequency current pulsing is illustrated in Fig. 1.

3.1.1 Low frequency pulsing

The cross-sectional macrographs of the bead profile, their penetration, width, aspect ratio and heat input are represented in Fig. 1. On examining the macrostructure, it is inferred that good quality welds with no surface / subsurface defects shall be obtained on employing PCGTA welding. Also it is witnessed that a maximum penetration of 3.9 mm could be achieved while employing the parameters indicated in trial 2. The heat input required for obtaining this penetration was found to be 691 J/mm. It was evident from the results that a penetration of $\geq$ 3 mm could be obtained in the five trials (Trial 2, 3, 4, 7 and 8). The minimum aspect ratio recorded was 3.51 in trial 2.

Fig. 1 Macrograph and Bead profile of high frequency and low frequency PCGTAW with penetration (P) in mm, width (W) in mm, depth to width ratio (W/P) and heat input (HI) J/mm.

3.1.2 High frequency pulsing

The macrostructure results of high frequency current pulsing portrayed that a full penetration of 4.03 mm could be achieved on employing the process parameters deployed in trial 5 with a heat input of 652 J/mm. The next higher value of penetration, 2.64 mm was obtained in trial 3 with heat input of 632 J/mm; followed by trial 9 having 2.42 mm depth with heat input of 630 J/mm. The least penetration of 1.73 mm was recorded in trial 1 with a heat input of 499 J/mm. The full penetration bead with minimum aspect ratio (3.29) is obtained in trial 5 and is represented in Fig. 2.

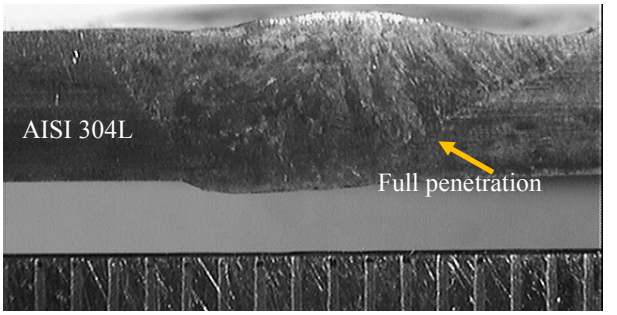

Fig.2 Full Penetration bead obtained in Trail no.5 of HF PC-GTAW AISI 304L

3.2 Taguchi Analysis

3.2.1. S/N ratio analysis and main effects plot

The signal to noise ratio analysis of the results was carried out to determine the optimized aspect ratio. As discussed in Section 2.1 lower the better criterion was selected for aspect ratio. The individual S/N ratio values of all the responses for each trial for both low and high frequency techniques are listed in Table 3 and 4. Average of S/N ratios at a corresponding level was calculated to find out the S/N ratio of each parameter level. The level of a factor with highest mean S/N value was chosen as the optimum level of the parameter irrespective of the criteria.

3.2.1.1 Low frequency pulsing

The main effects plots for the S/N ratios are shown in Fig. 3a. The response table of the S/N values of aspect ratio is shown in Table 5. From the response table and main effect plots, combination of optimum level of the parameters was interpreted. Peak % followed by frequency was the most significant factors which determine the aspect ratio. From the main effects plot, mean S/N values of aspect ratio is inversely proportional to I_P from level 1 to level 2 and directly proportional, when I_P is increased from level 2 to 3 as observed in Fig. 3a.With an increase in I_B, pulse on time % and frequency from level 1 to 2, mean S/N value was found to increase and then decreases with a from level 2 to 3. The optimized parameters for lower aspect ratio are shown in Table 6.

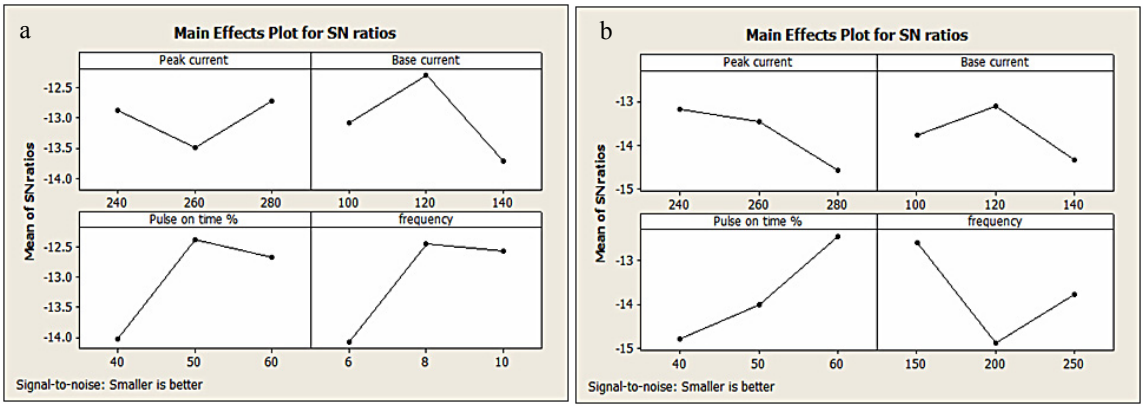

Fig.3 Main Effects plot for S/N ratios of Aspect Ratio for (a) LF-PCGTAW (b) HF-PCGTAW

3.2.1.2. High frequency pulsing

The mean S/N values of the Aspect Ratio (W/P) for each level of the parameters are represented in Table 7. On analyzing the mean S/N values on the response table, it is well noticed that Aspect Ratio was affected mostly by peak %, frequency, I_P and I_B in decreasing order of significance. The optimized levels of the parameters are shown in Table 8.

Table 5 Response table representing S\ N values of Aspect Ratio (AR) for LF-pulsing

Level	Peak current	Base current	Peak %	Frequency
1	-12.88	-13.08	-14.04	-14.07
2	-13.49	-12.29	-12.38	-12.45
3	-12.72	-13.72	-12.67	-12.57
Delta	0.77	1.43	1.65	1.63
Rank	4	3	1	2

Table 6 Optimized parameters for lower aspect ratio (AR) in LF-pulsing

S. No	Factor	Level	Values
1	Peak current(A)	3	280
2	Base current(A)	2	120
3	Peak %	2	50
4	Pulse frequency	2	8

Table 7 Response table representing S/N values of Aspect Ratio (AR) for HF-pulsing

Level	Peak current	Base current	Peak %	frequency
1	-13.19	-13.77	-14.79	-12.58
2	-13.47	-13.12	-14.01	-14.88
3	-14.58	-14.35	-12.44	-13.78
Delta	1.39	1.23	2.35	2.31
Rank	3	4	1	2

Table 8 Optimized parameters for lower Aspect Ratio (AR) in HF-pulsing

S. No	Factor	Level	Values
1	Peak current(A)	1	240
2	Base current(A)	2	120
3	Peak %	3	60
4	Pulse frequency	1	150

The main effects plots of the same parameters in order are shown in Fig. 3b. It was witnessed that mean S/N values for Aspect ratio (W/P) was found decreasing from levels 1 to 3 in the case of I_P. With an increase in I_B, the mean S/N value was found to increase to a peak value from level 1 to 2 and then it decreased from level 2 to 3. Also, on increasing the peak % in HF current pulsing, the mean S/N value also increased. The mean S/N value decreased initially and then increased with increase in frequency.

3.3 Analysis of Variance (ANOVA)

ANOVA was done at 5 % level of significance to identify the significance and percentage contribution of each factor on the bead geometry (W/P) of AISI 304 L. The four parameters which are used in ANOVA are the Degree of Freedom (DOF), Sum of squares (SS), Variance (V) and percentage contribution to the total variation which can be calculated using the equations (4-8) [14] given below.

$$SS_T = \sum_i^m \eta_i^2 - \frac{1}{m}\left[\sum_{i=1}^m \eta_i\right]^2 \quad (4)$$

SS_T is the total sum of squares, m is total number of experiments, η_i is the S/N ratio of the i^{th} test.

$$SS_p = \sum_{j=1}^{t} \frac{(S_{\eta_j})^2}{t} - \frac{1}{m}\left(\sum_{i=1}^m \eta_i\right)^2 \quad (5)$$

SS_P is Sum of squares of the tested factors, p represents one of the tested factors, j is level of this specific factor p ,t- repetition of each level of S_{η_j} factor p, is the sum of S/N ratio involving this factor and level j

$$V_P(\%) = \frac{SS_P}{D_P} \times 100 \quad (6)$$

V_P - the variance from the tested factors, D_P - Degree of freedom of each factor .

$$SS'_P = SS_P - D_P V_E \quad (7)$$

SS'_P - Corrected sum of squares from the tested factors, V_E - Variance for the error

$$P_P(\%) = \frac{SS_P{}'}{SS_T} \times 100 \quad (8)$$

$P_P(\%)$- Percentage contribution of each individual factor to the total variation

3.3.1 Low frequency Pulsing

ANOVA results of the low frequency PCGTAW for Aspect ratio is shown in Table 9. Percentage contribution of each factors on the responses are calculated and are shown in Fig. 4a The aspect ratio was mostly influenced by peak percentage which was 36% then followed by pulse frequency (35 %), I_B (21 %) and I_P (6 %).

3.3.2 High frequency pulsing

The results of ANOVA on the high frequency PCGTAW for aspect ratio are shown in Table 10. Percentage contribution of each factors on the responses are found and are shown in Fig 4b. Peak % had 39% influence on aspect ratio then by frequency with almost same significance of 36% followed by I_P (14%) and I_B (10%). Fig. 4 ANOVA results showing Percentage contribution of each factor for aspect ratio (AR) in a) Low Frequency b) High frequency

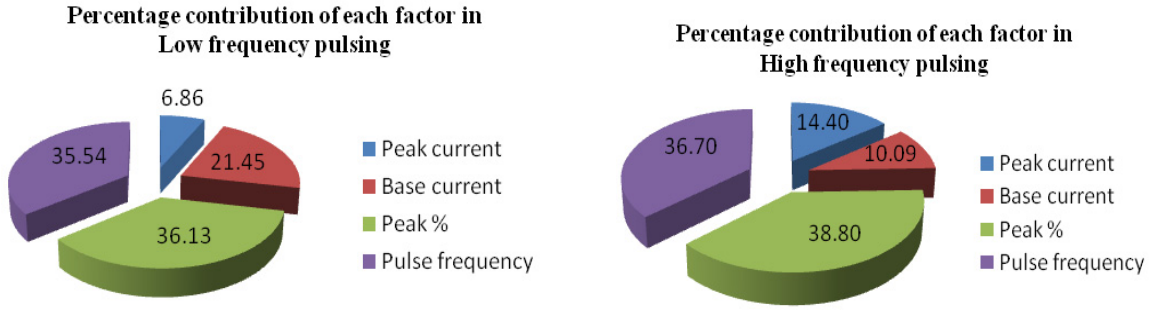

Fig.4. ANOVA results showing Percentage contribution of each factor for aspect ratio (AR) in a) Low Frequency b) High frequency

4. Discussion

On comparing the results of both low and high frequency current pulsing techniques, it is well observed that on employing higher welding speed and also at higher frequencies the arc is more focused in HF-PCGTAW. Further, the high frequency pulsed GTA process has better control over the maximum penetration with minimum heat input than that of low frequency which is evident from Giridharan et al. [4]. They reported that the maximum depth of 3.85 mm with a heat input of 970 J/mm. The major achievement of this work is enhanced weld penetration up to 4.03mm with reduced (36%) heat input of

Table 9 ANOVA Results for aspect ratio AR for LF-pulsing

Factors	Degree of freedom (DOF)	Sum of Squares (SS)	Variance (V)	Corrected sum of squares ss'	Contribution (%)	Rank
Peak current	2	0.256	0.128	0.256	6.86	4
Base current	2	0.800	0.400	0.800	21.45	3
Peak %	2	1.347	0.674	1.347	36.13	1
Pulse frequency	2	1.325	0.663	1.325	35.54	2
Error	0	0	0	0	0	
Total	8	3.728			100	

Table 10 ANOVA Results of Aspect ratio for HF-pulsing

Factors	Degree of freedom (DOF)	Sum of Squares (SS)	Variance (V)	Corrected sum of squares ss'	Contribution (%)	Rank
Peak current	2	0.932	0.466	0.932	14.40272	3
Base current	2	0.653	0.327	0.653	10.09118	4
Peak %	2	2.511	1.256	2.511	38.80389	1
Pulse frequency	2	2.375	1.187	2.375	36.70221	2
Error	0	0	0	0	0	
Total	8	6.471			100	

625J/mm. The faster the pulsing, the greater is the travel speed which would result in better weld qualities. This is the reason attributed to the difference in welding speed in both the techniques. Thus on using higher frequency, less time would be spent for welding in a particular region which in turn reduces the heat input. Hence in HF-PCGTAW, energy is saved considerably thereby enhancing the productivity. Reducing the heat input from the fusion zone limits formation of undesirable phases and thus improves the weld properties. It is observed that full penetration of 4 mm is achieved in trial 5 whereas rest of the trials showed substantially less penetration. Also on closer examination, it could be inferred that the frequency of 150 Hz has played significant variations in the depth of penetration with respect to the variations in the parameters from trials 1, 5 and 9 as represented in Table 4.The wide range of frequency is chosen in the case of high pulsing in order to find out the possible range for good penetration. It is suggested that further investigations with frequency trials around the close range of 150 Hz might give better penetration. The bead width in high frequency pulsed weld was found to be lower than that of the low frequency pulsed welds (Table 3-4).

On comparing the main effects plots of low and high frequency PCGTAW, it was observed that the I_B plots had almost the same pattern for both the techniques Fig. 3(a-b).This was due to the fact that effect of base current is only to maintain a stable arc. Trend of main effects plot of the other three parameters are different in low and high frequency PCGTAW. Peak current pulse would be remain ON for a longer time if peak % is more. As the heat required for melting the base metal is supplied during the peak pulse, more heat will be transferred when peak % is more. This in turn results in good penetration and higher bead width. This is the reason peak % is the most influencing parameter which is also witnessed in Fig. 4. Higher value of peak % (60%) is required in HF- pulsing since the speed at which pulsing occur is more which has to be compensated with more peak % to get a good penetration than in LF- pulsing (50%) which can be validated from the Table 6 and 8.

5. Conclusions

The present study investigates the use of low and high frequency current pulsing for welding 4 mm thick AISI 304L plates. Lower the better criterion was used to analyze results of aspect ratio. The outcomes of the work have been deduced as concluding summary and are reported as follows.

1. Full penetration of 4mm was achieved in the high frequency pulsing with a process parameter combination of I_P = 260 A, I_B= 120 A, Peak %= 60 and frequency=150 Hz.
2. Full penetration was obtained in trial 5 of high frequency pulsing (Fig. 2) with a heat input of 652 J/mm. whereas, in low frequency pulsing trail 3 and 4 the penetration was lower (3 mm and 3.05 mm)respectively with a heat input of 672 J/mm and 669 J/mm.. From this it is evident that the heat input in HF pulsing is comparatively lesser.
3. In HF pulsing the Peak % ON time is the factor which has most influence on the bead geometry while in low frequency pulsing the frequency (Hz) influences the most.

Acknowledgement

The authors sincerely thank Aeronautical Research and Development Board (AR&DB), India for providing the financial aid towards this research work.

References

[1] Viswanathan R and Bakker W (2001) Materials for Ultra supercritical Coal Power Plants-Boiler Materials: Part 1, J Mater Eng Perform. 10:81-95.

[2] Baddoo NR (2008) Stainless steel in construction- A review of research, applications, challenges and opportunities. J of Constructional Steel Research. 64:1199-06.

[3] Lippold JC and Koteki DJ (2005) Welding Metallurgy and Weldability of Stainless steels 2nd ed. New Jersey: John Wiley & Sons.

[4] Giridharan PK, Murugan N (2009) Optimization of pulsed GTA welding process parameters for the welding of AISI 304L stainless steel sheets. Int J Adv Manuf Technol. 40:478–489.

[5] Karunakaran N, (2012) Effect of Pulsed Current on Temperature Distribution, Weld Profiles and Characteristics of GTA Welded Stainless Steel Joints. Int J Engineering and Technology. 2:1908-1916.

[6] Martin L (2014) The Avesta welding manual- practice and products for stainless steel welding. Avesta welding AB, Sweden. www.kskct.cz/images/materialy/en/avesta/.pdf

[7] Yousefieh M, Shamanian, M, Saatchi A (2011) Influence of Heat Input in Pulsed Current GTAW Process on Microstructure and Corrosion Resistance of Duplex Stainless Steel Welds. J. Iron and Steel Research International 18(9):65-69.

[8] Kou S, Le Y, (1986) Nucleation mechanism and grain refining of weld metal.Welding Journal. American welding society and the welding research council. 65:305-313.

[9] Tseng KH, Chou CP (2002) The effect of pulsed GTA welding on the residual stress of a stainless steel weldment. J Materials processing Technology. 123:346-353.

[10] Farahani F ,Shamanian F, Ashrafizadeh A (2012) Comparative study on direct and pulsed current gas tungsten arc welding of Alloy 617. AMAE Int J Manufacturing and Material Science. 02 (01):1-6.

[11] Yousefieh M,Shamanian M, Arghavan AR (2012) Analysis of Design of Experiments Methodology for Optimization of Pulsed Current GTAW Process Parameters for Ultimate Tensile Strength of UNS S32760 Welds. Metallogr Microstruct Anal 1: 85–91.

[12] Balasubramanian M, Jayabalan V, Balasubramanian V(2010) Effect of process parameters of pulsed current tungsten inert gas welding on weld pool geometry of titanium welds. Acta Metallurgica. Sinica.(English Letters).23(4):312-320.

[13] Babu S, Senthil kumar T, Balasubramanian V (2008) Optimizing pulsed current gas tungsten arc welding parameters of AA6061 aluminium alloy using Hooke and Jeeve's algorithm. Trans. Nonferrous Met. Soc. China 18:1028-1036.

[14] Yousefieh M, Shamanian M, Saatchi A (2011) Optimization of the pulsed current gas tungsten arc welding (PCGTAW) parameters for corrosion resistance of super duplex stainless steel (UNS S32760) welds using the Taguchi method. J Alloys and Compounds 509: 782-788.

[15] Padmanban G, Balasubramanian V (2011) Optimization of pulsed current gas tungsten arc welding process parameters to attain maximum tensile strength in AZ31B magnesium alloy. Trans. Nonferrous Met. Soc. China 21:467-476.

[16] Technical Information (2014) Superior for Stainless: High-Speed Pulsed GTAW Boosts Productivity, Quality while Reducing Distortion. http://www.millerwelds.com/resources/articles/ Superior-Stainless-High-Speed-Pulsed-GTAW-Boosts-Productivity-Quality-Reduce-Distortion/. Accessed 05/07/2014